Supporting Information

Room temperature precipitated dual phase $CsPbBr_3$-$CsPb_2Br_5$ nanocrystals for stable perovskite light emitting diodes

Bai-Sheng Zhu,[a, b] Huai-Zhi Li,[a, b] Jing Ge,[a, c] Hao-Dong Li,[a, b] Yi-Chen Yin,[a, b] Kun-Hua Wang,[a, b] Chen Chen,[a, b] Ji-Song Yao,[a, b] Qun Zhang,[a, c] Hong-Bin Yao*[a, b, d]

[a]Division of Nanomaterials & Chemistry, Hefei National Research Center for Physical Sciences at the Microscale, [b]Department of Applied Chemistry, [c]Department of Chemical Physics, [d]Hefei Science Center of CAS, University of Science and Technology of China, Hefei, Anhui 230026, China
E-mail: yhb@ustc.edu.cn
Group website: http://staff.ustc.edu.cn/~yhb/

Materials and Chemicals. Lead bromide ($PbBr_2$, Aladdin, 99.99%), cesium bromide (CsBr, Aladdin, 99.99%), di-dodecyl dimethyl ammonium bromide (DDAB, Energy Chemical, 98%), octane (Alfa Aesar, anhydrous 99%), hexylamine (Afla Aesar, 99%), hydrogen bromide (HBr, SCRC, AR), oleic acid (OA, Afla Aesar, 90%), oleylamine (OAm, Aldrich, 70%), octadecene (ODE, Aldrich, 90%), cesium carbonate (Cs_2CO_3, Afla Aesar, 99.99%), butylamine (BuAm, Aladdin, 99.5%), 2-propanol (IPrOH, SCRC, AR), propionic acid (PrAc, SCRC, AR), n-hexane (HEX, SCRC, AR), toluene (SCRC, AR), chlorobenzene (Acroseal, anhydrous 99.8%), methanol (SCRC, AR), trioctylphosphine oxide (TOPO, Aldrich), poly(3,4-ethylenedioxythiophene):poly(styrenesulfonate) (PEDOT : PSS, Al4083 Clevios), poly(9-vinlycarbazole) (PVK, Aldrich), poly(N,N’-bis(4-butylphenyl)-N,N’-bis(phenyl)-benzidine) (poly-TPD, Xi’an Polymer Light Technology Corp.), 2,4,6-Tris(3-(diphenylphosphinyl)phenyl)-1,3,5-triazine (PO-T2T, Nichem).

Preparation of $C_6H_{13}NH_3Br$ (HABr). 25 mL of methanol and 10 mL of hexylamine were loaded and stirred in a 250 mL of flask under an ice water bath. After the dropwise addition of HBr (13 mL) into the mixture, the ice water bath was removed and the mixture was stirred for 2 hours at room temperature. The product was obtained by a rotary evaporator at 70 °C to remove solvent. Then the material was washed by diethyl ether and subsequently recrystallized from a mixture of diethyl ether and ethanol. After filtration, the product was collected and dried under vacuum at 60 °C for 24 hours. The obtained HABr was stored in a glovebox.

Tables and Figures

Table S1 Fitted (by three-exponential fit) PL lifetimes of all inorganic Cs-Pb-Br perovskites films after annealing at different temperatures.

	Temperature (^{o}C)	**τ_1 (ns)**	**f_1 (%)**	**τ_2 (ns)**	**f_2 (%)**	**τ_3 (ns)**	**f_3 (%)**	**τ_{avg} (ns)**
HI	25	1.03	27.93	4.35	41.91	21.98	30.16	8.74
	50	0.99	31.49	4.11	40.71	22.18	27.80	8.15
	100	0.66	44.35	3.24	35.60	20.60	20.05	5.57
	150	0.70	49.99	3.47	30.70	20.23	19.31	5.32
	200	-	-	-	-	-	-	-
LARP-SP	25	0.72	24.44	3.64	38.27	19.93	37.29	9.00
	50	0.74	32.43	3.90	34.68	21.34	32.89	8.61
	100	0.53	32.02	3.02	32.69	18.63	35.29	7.96
	150	0.49	38.33	3.17	28.39	20.64	33.28	7.73
	200	-	-	-	-	-	-	-
LARP-DP	25	0.88	22.3	4.18	43.7	17.81	34	8.08
	50	0.54	9.69	5.17	21.83	27.21	68.48	19.81
	100	0.85	1.65	5.81	15.65	36.66	82.7	31.24
	150	0.47	3.5	5.23	10.91	38.86	85.59	33.84
	200	0.38	6.34	5.08	9.63	43.54	84.03	37.01

The measured values were fitted to the equation [2]:

$$f(t) = A_1 \exp\left(-\frac{t}{\tau_1}\right) + A_2 \exp\left(-\frac{t}{\tau_2}\right) + A_3 exp(-\frac{t}{\tau_3})$$

The average lifetimes were calculated using:

$$\tau_{avg} = (A_1\tau_1^2 + A_2\tau_2^2 + A_3\tau_3^2)/(A_1\tau_1 + A_2\tau_2 + A_3\tau_3)$$

Where τ_1 is a short-lived PL lifetime, τ_2 is an intermediate PL lifetime, and τ_3 is a long-lived PL lifetime. For

HI and LARP-SP NCs films, annealing treatment may cause part loss of surface ligand, leading more surface and trapping states on NCs, which thus resulted in the increase of fraction of short-lived PL lifetime (f_1) and intermediate PL lifetime (f_2), which makes a contribution to the slight reduction of the average lifetime τ_{avg}. However, in dual-phase $CsPbBr_3$-$CsPb_2Br_5$ perovskites films, $CsPb_2Br_5$ nanoplatelets would passivate the surface of $CsPbBr_3$ NCs with shallow interfacial traps. At room temperature, these trapped excitons can be thermally ionized followed by the formation of radiative excitons, which would promote the multiple excitons recombination. These shallow traps, essentially participate in the photoluminescence processes and can be considered to be in the bright state (PL active), which would cause the increase of the fraction of long-lived PL lifetime with the enhancement of annealing temperature.

Table S2 Details of EL spectral stability of devices based on LARP-DP under 5.5 V continuous voltage operation.

Time (min)	**EL (nm)**	**FWHM (nm)**
0	518	19.28
20	518	19.36
40	518	19.38
60	518	19.22
80	518	19.33
100	518	19.30
120	518	19.20

Table S3 Details of EL spectral stability of devices based on HI (a) or LARP-SP (b) continuously operated at 5.5 V.

a

Time (min)	**EL (nm)**	**FWHM (nm)**
0	517	18.18
40	517	18.86
80	518	19.41
120	519	19.88
160	520	20.33
200	522	21.26
240	523	21.83

b

Time (min)	**EL (nm)**	**FWHM (nm)**
0	518	19.47
10	518	19.82
20	519	20.27
30	520	20.69
40	521	21.14
50	522	21.93
60	524	22.71

Table S4 A comparison of our device with other previously reported green PeLEDs mainly based on LARP-NCs.

Emitter Type	**Synthetic Method**	**Synthetic Condition**	**Ligand**	**Surface Roughness (nm)**	**Lmax (Cd m^{-2})**	**EL (nm)**	**EQE (%)**	**Turn-on Bias (V)**	**Ref.**
$CsPbBr_3$ - Cs_4PbBr_6	Polycrystalline film technology	N_2; RT; DMSO	-	-	1150	514 ~ 522	2.4×10^{-3}	3.0 ~ 4.0	3
$CsPbBr_3$	Polycrystalline film technology	N_2; RT; DMSO	-	-	13752	522	1.37	3.0 ~ 3.5	4
$CsPbBr_3$	HI	N_2; 140-200 °C; ODE	OA; OLA	-	330	515	3.0	3.0	5
$CsPbBr_3$	HI	N_2; 140-200 °C; ODE	OA; OLA	-	15185	512	6.27	3.4	6
$CsPbBr_3$ - $CsPb_2Br_5$	HI	Ar; 130 °C; ODE	OA; OLA	3.2	3853	527	2.21	4.5 ~ 5.0	7
$CsPb_2Br_5$	LARP	N_2; DMSO; Toluene	HABr	5	7317	520	1.1	3.8	8
FA-$CsPbBr_3$	LARP	Air; RT; Toluene	TOAB; DDAB; OTAc	2.3	55800	515	11.6	2.75	9
$CsPbBr_3$	LARP	Air; RT; DMF; Toluene	OA; TOAB	-	110	515	1.5×10^{-2}	3.2	10
$CsPbBr_3$	LARP	Air; RT; Water; DMF; Toluene	OA; OLA	-	4428	518	1.7	3.0 ~ 4.0	11
$CsPbBr_3$ -$CsPb_2Br_5$	**LARP**	**Air; RT; Methanol; DMF; Toluene**	**HABr; DDAB**	**20**	**8383**	**518**	**0.62**	**2.5**	**This work**

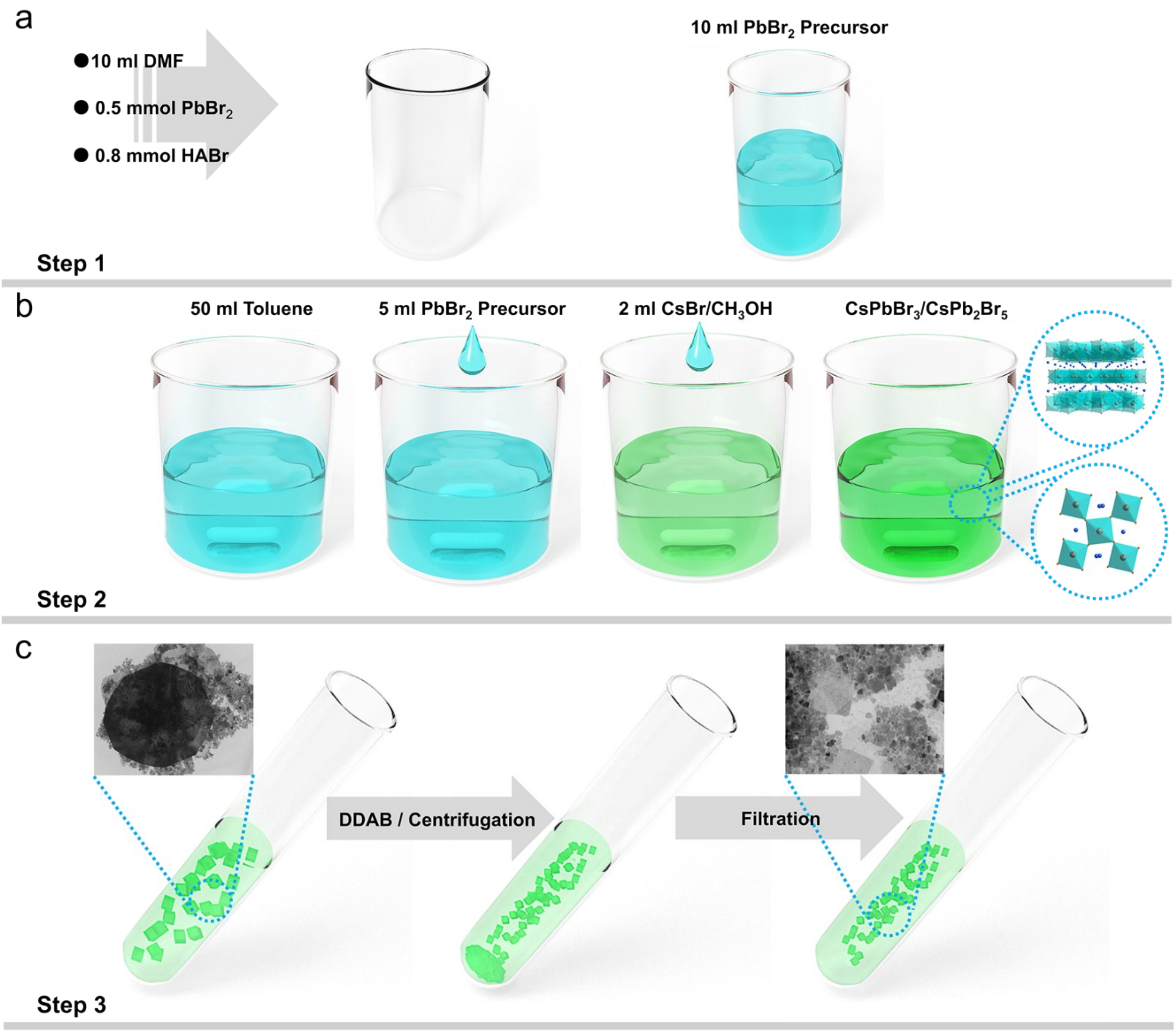

Fig. S1 Schematic illustration of synthetic procedure of dual phase $CsPbBr_3$-$CsPb_2Br_5$ NCs carried out by LARP approach. (a) Preparison of $PbBr_2$ precursor. (b) Synthetic procedure of dual phase $CsPbBr_3$-$CsPb_2Br_5$ NCs. (c) Separation of dual phase $CsPbBr_3$-$CsPb_2Br_5$ NCs. After DDAB/Centrifugation treatment, the resulted supernatant without being further filtered through 0.45 μm nylon filter, was also collected for XRD characterizations. The corresponding PXRD pattern of dual phase $CsPbBr_3$-$CsPb_2Br_5$ NCs without filteration treatment was provided in Fig S2.

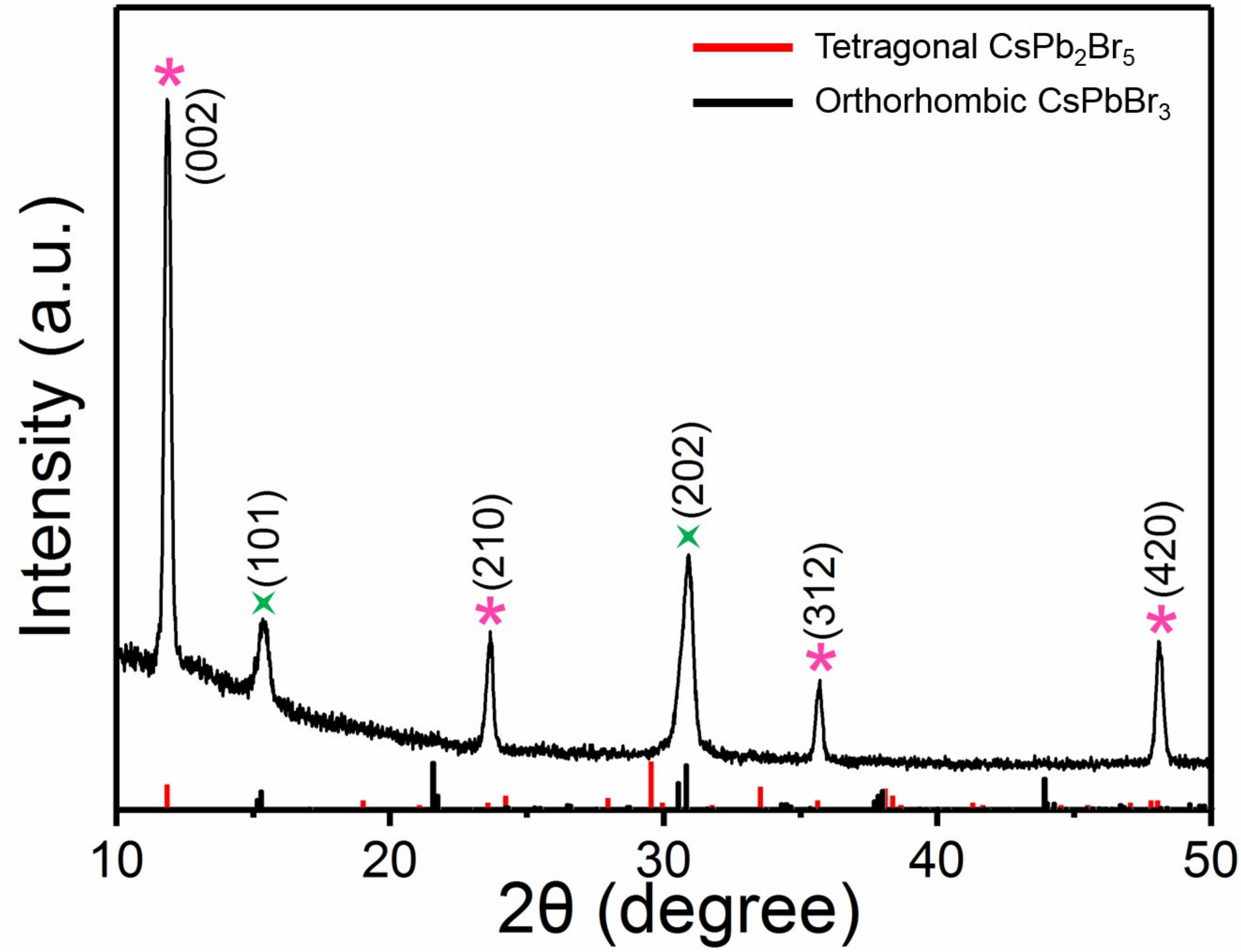

Fig. S2 PXRD pattern of dual phase CsPbBr$_3$-CsPb$_2$Br$_5$ NCs (without being filtered through 0.45 μm nylon filter), together with standard pattern of orthorhombic CsPbBr$_3$ (black line, (*Pnma*) space group) and tetragonal CsPb$_2$Br$_5$ (red line, (*I4/mcm*) space group). The PXRD pattern was collected on Si wafer.

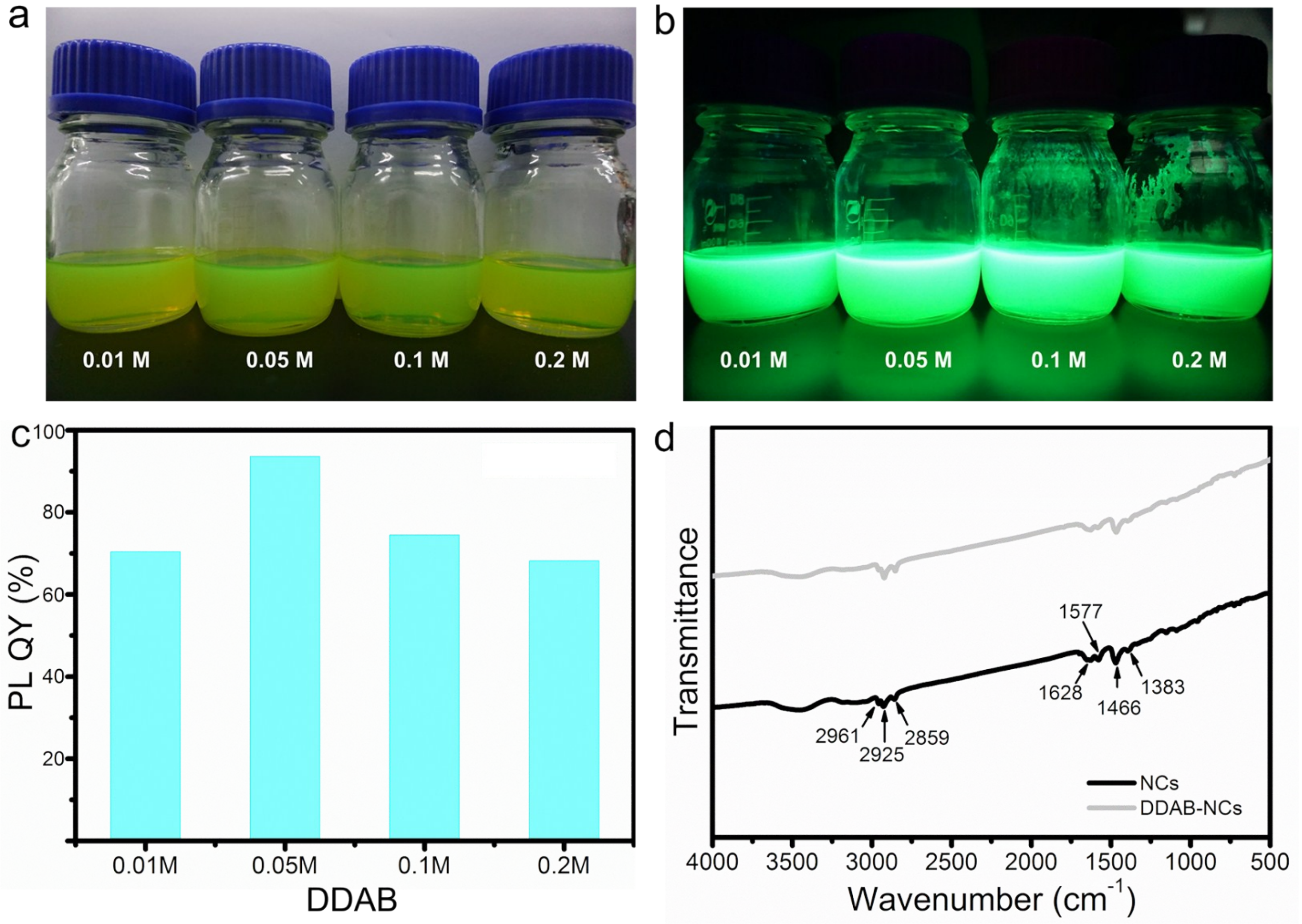

Fig. S3 Photographs of $CsPbBr_3$-$CsPb_2Br_5$ colloidal NCs solution treated with various concentration of DDAB under daylight (a) and a UV light irradiation (b), respectively. (c) Absolute PLQYs of samples treated with various concentration of DDAB. (d) Fourier transform infrared (FTIR) spectra of as-synthesized $CsPbBr_3$-$CsPb_2Br_5$ NCs and the NCs treated with 0.05 M DDAB (dosage of DDAB during treatment is considerably low). FTIR was used to examine the presence of ligands on as-synthesized and DDAB treated $CsPbBr_3$-$CsPb_2Br_5$ NCs,[1] both samples show CH_2 and CH_3 symmetric and asymmetric stretching vibrations in the range of 2859-2961 cm^{-1}, and CH_2 bending vibration at 1466 cm^{-1}. Peak at 1628 cm^{-1} can be ascribed to the asymmetric NH_3^+ deformation.There was almost no obvious change in peak intensity before and after DDAB treatment, indicating a little ligand-exchange process occurred between HABr and DDAB on the surface of $CsPbBr_3$-$CsPb_2Br_5$ NCs.

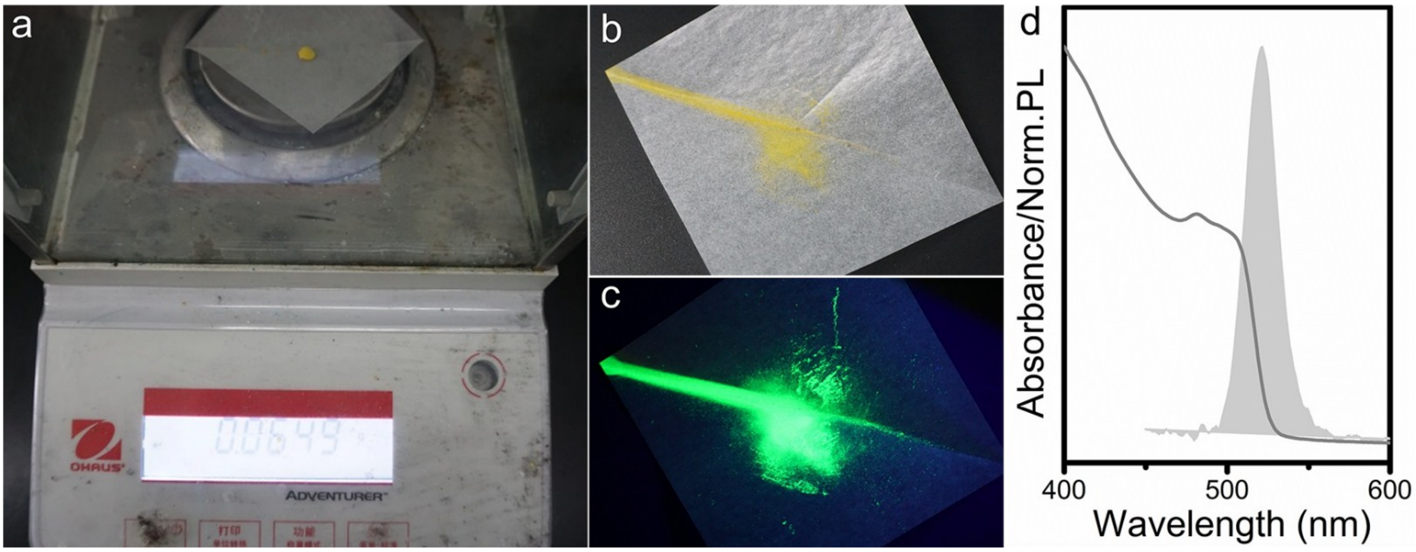

Fig. S4 Photographs of large scale synthesized dual phase $CsPbBr_3$-$CsPb_2Br_5$ powder (a,b) under ambient conditions and (c) under UV light (365 nm) irradiation. (d) UV-Vis absorption (left) and PL (right) spectrum of $CsPbBr_3$-$CsPb_2Br_5$ NCs film coated on a glass slide.

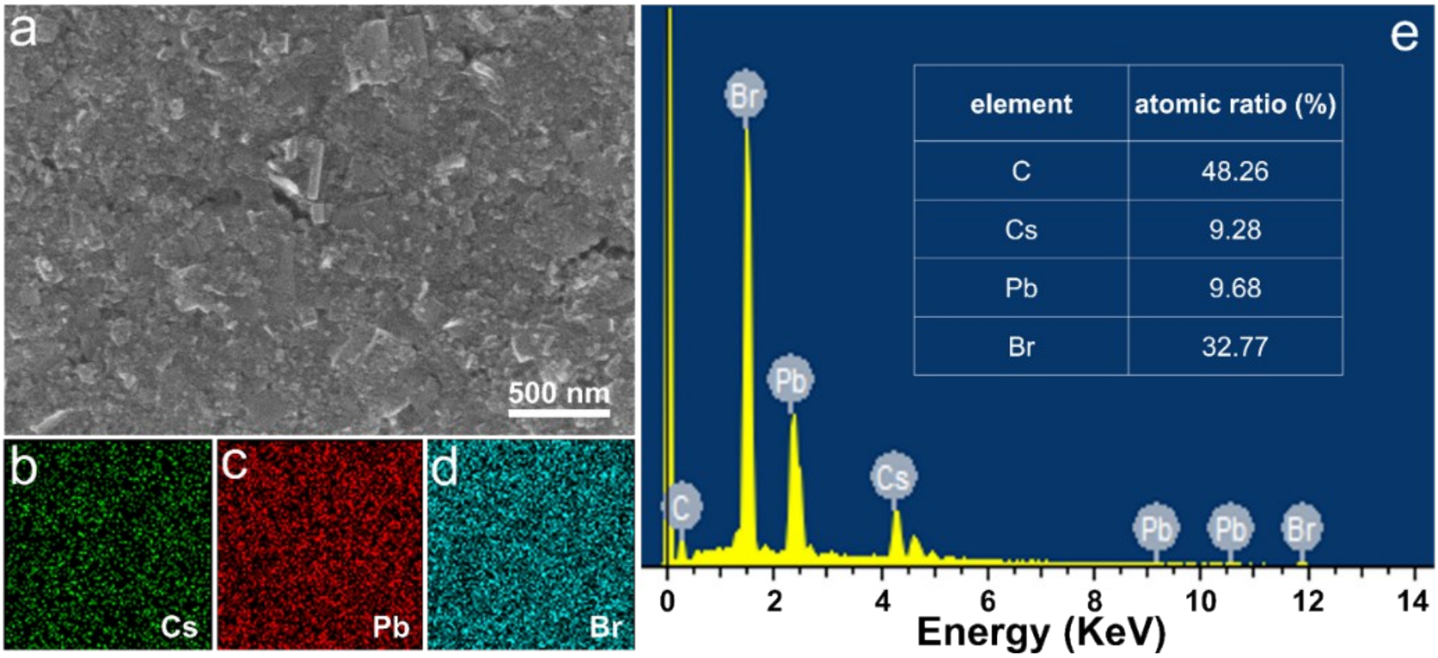

element	atomic ratio (%)
C	48.26
Cs	9.28
Pb	9.68
Br	32.77

Fig. S5 (a) Typical SEM image of $CsPbBr_3$-$CsPb_2Br_5$ NCs film. Elemental mapping images of the dual phase $CsPbBr_3$-$CsPb_2Br_5$ NCs film, showing the elemental distribution of (b) Cs, (c) Pb, and (d) Br. (e) Energy Dispersive X-ray Spectroscopy (EDS) of the dual phase $CsPbBr_3$-$CsPb_2Br_5$ NCs film. Quantification of the EDS spectrum reveals a Cs: Pb: Br atomic ratio of 1:1.04:3. 53.

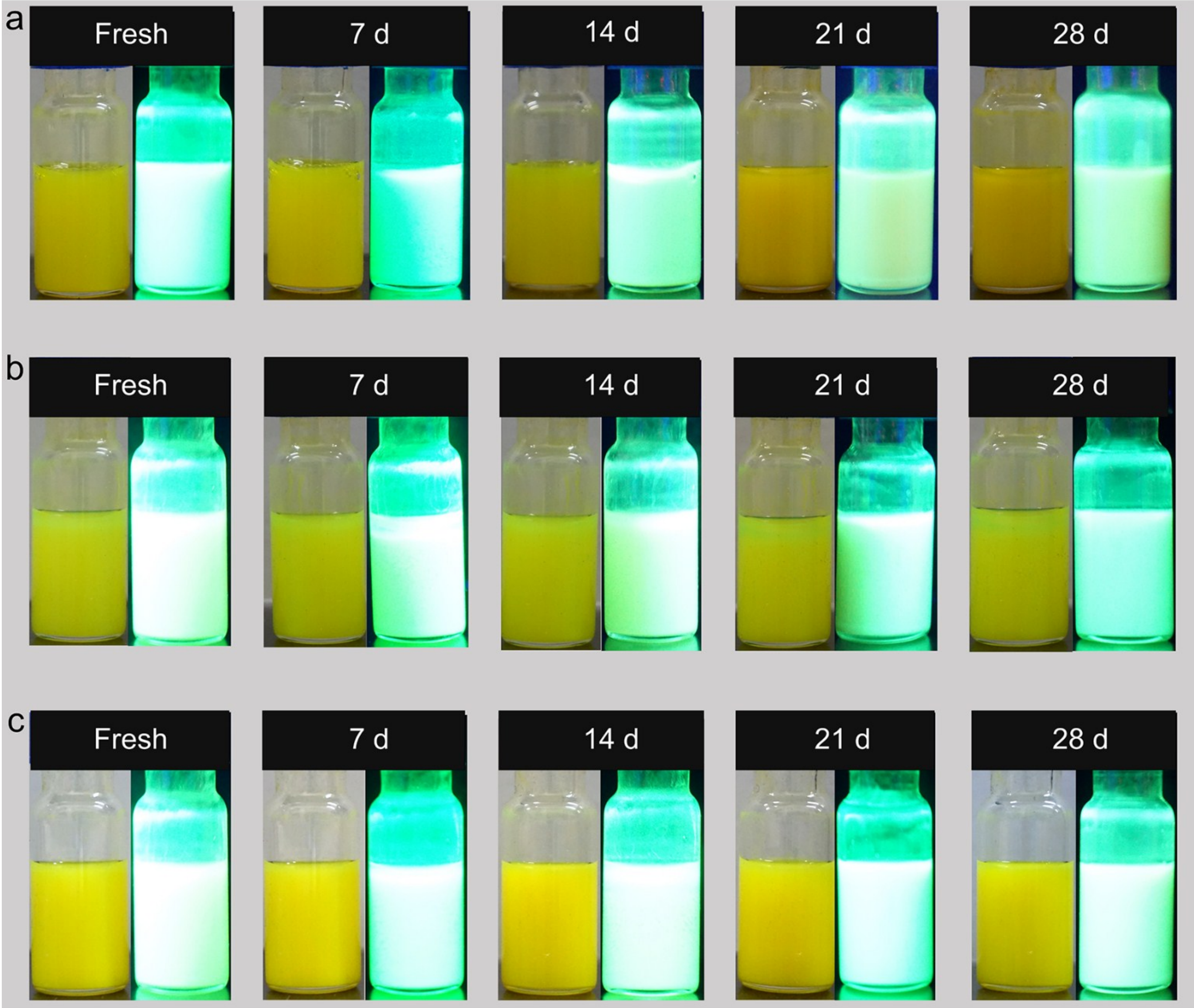

Fig. S6 Photographs for all inorganic Cs-Pb-Br perovskite NCs dispersed in toluene taken at daylight or upon 365-nm UV light irradiation during 4 weeks. Vials from top to down are corresponding to the samples synthesized by (a) HI, (b) LARP-SP and (c) LARP-DP, respectively. It can be seen that the samples synthesized through LARP-DP (c) remain essentially unchanged within 28 days, which markedly differentiates from the phenomena of HI NCs (a) and LARP-SP NCs (b) that underwent a rapid degradation in terms of dispersion color and light emitting under UV light irradiation.

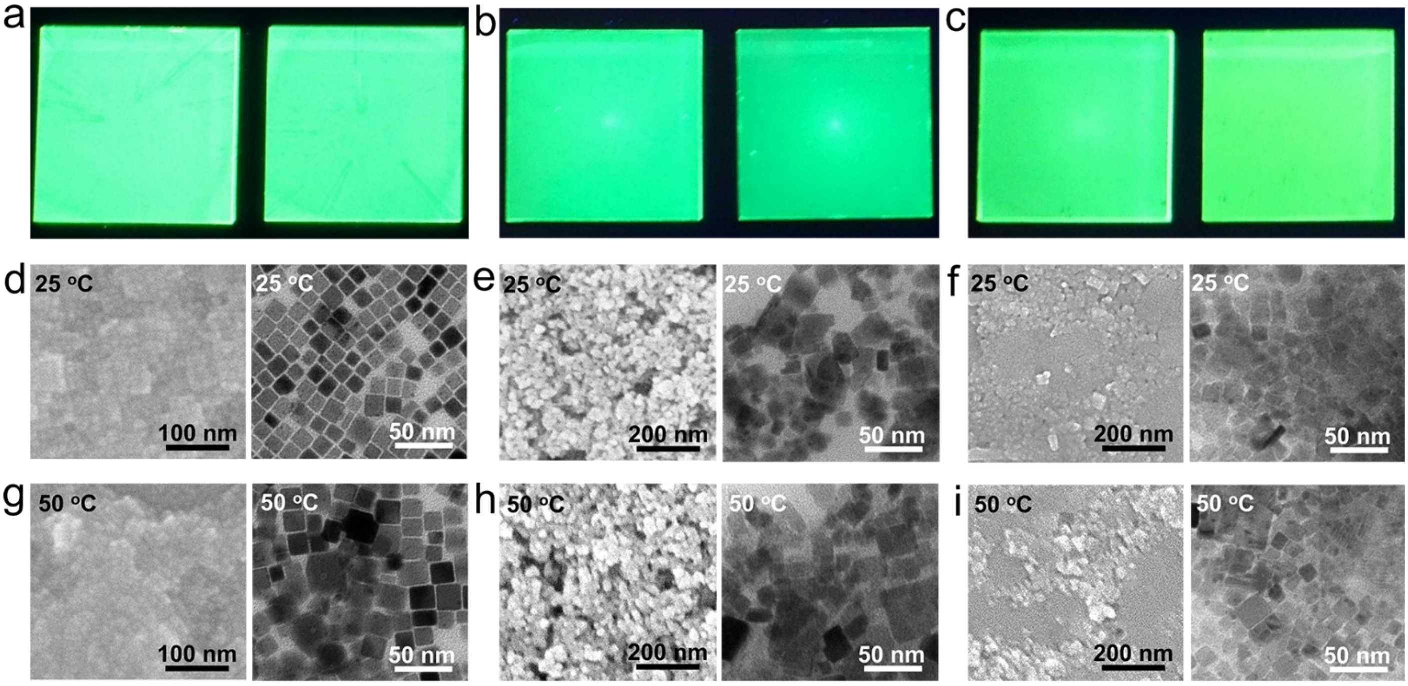

Fig. S7 PL emission photographs, typical SEM and TEM images of all inorganic Cs-Pb-Br perovskite NCs films ((a), (d), (g) for HI, (b), (e), (h) for LARP-SP, (c), (f), (i) for LARP-DP) after annealing at 25 and 50 ºC under ambient conditions, respectively.

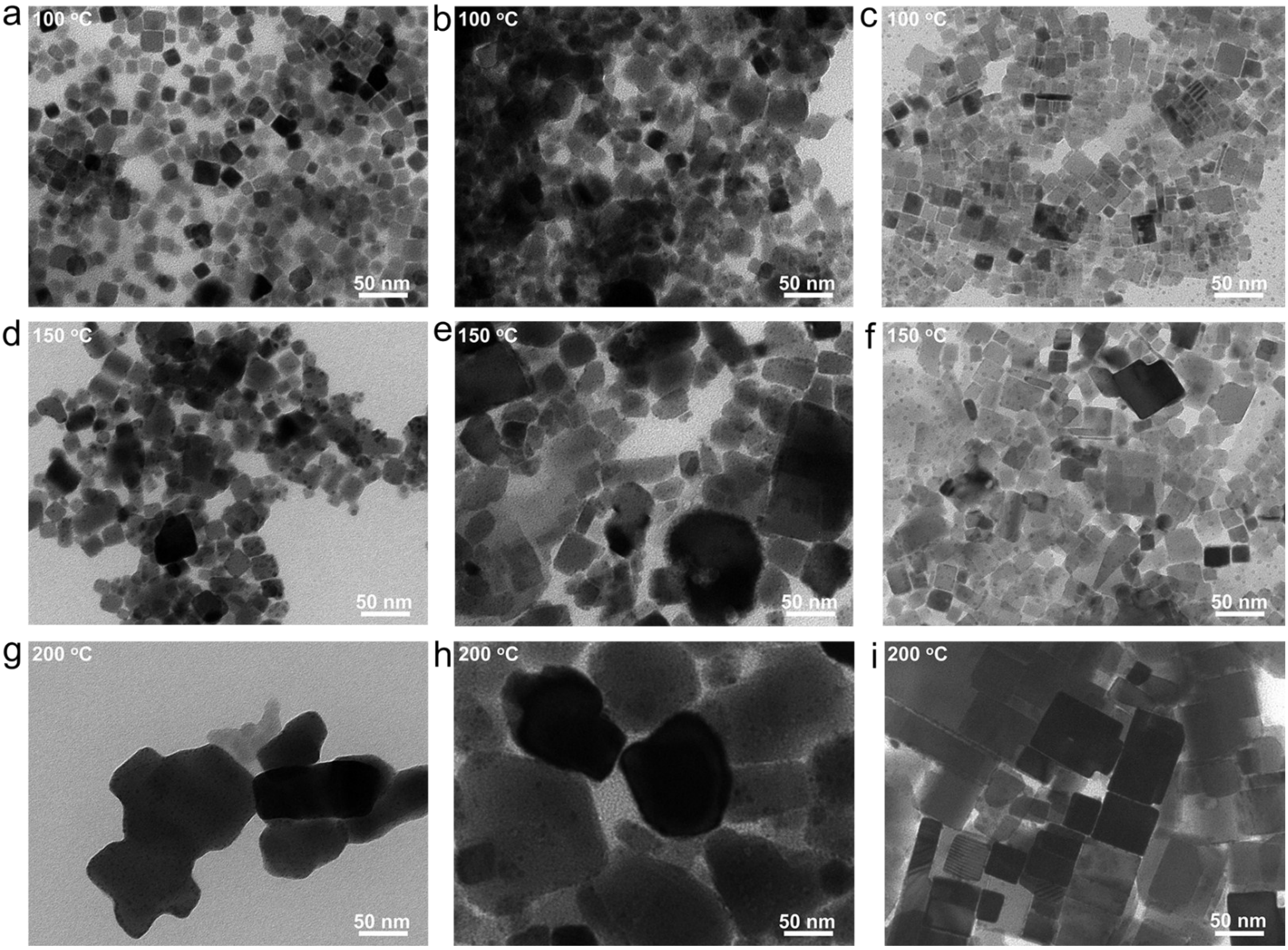

Fig. S8 TEM images of all inorganic Cs-Pb-Br perovskite NCs after annealing at 100, 150 and 200 ºC in air atmosphere, respectively. (a), (d) and (g) refer to HI; (b), (e) and (h) refer to LARP-SP; (c), (f) and (i) refer to LARP-DP, respectively.

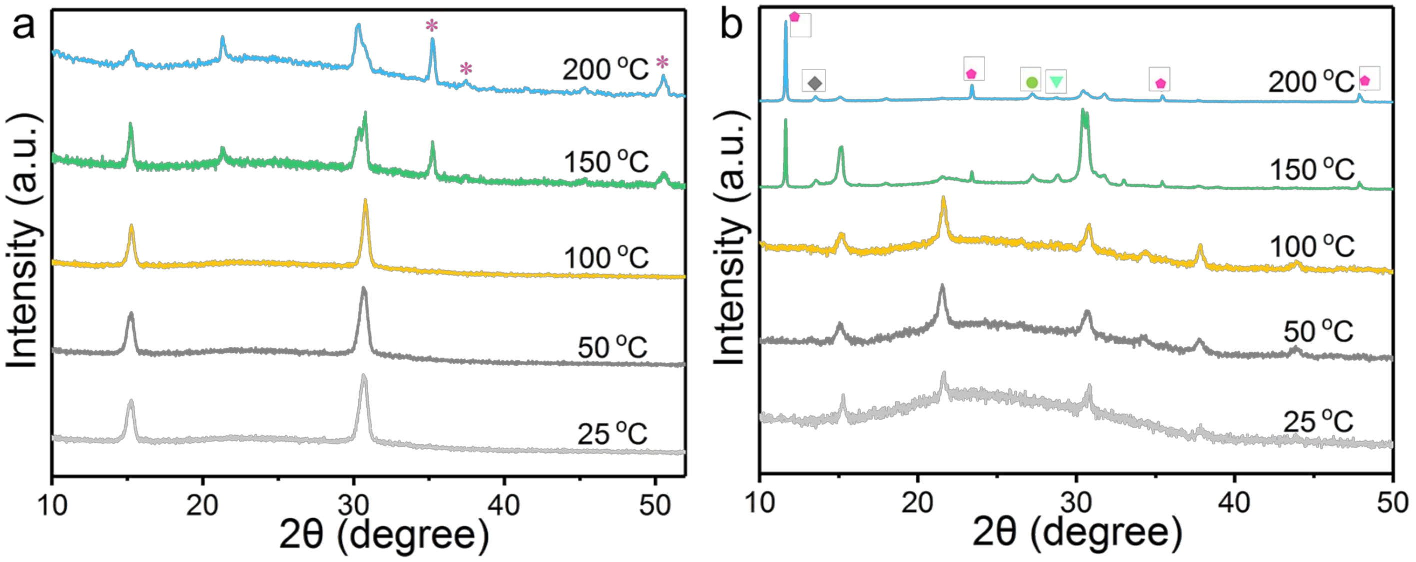

Fig. S9 *Ex situ* PXRD patterns of HI-cubic $CsPbBr_3$ (a) and LARP-SP orthorhombic $CsPbBr_3$ (b) annealed at different temperatures between 25 and 200 ºC in air environment. The cubic $CsPbBr_3$ and orthorhombic $CsPbBr_3$ was synthesized by HI and LARP-SP, respectively. The stars in (a) denoted the presence of Pb_2OBr_2 ($2\theta = 35.2°$), and $PbCO_3$ ($2\theta = 37.4°, 39.6°$). In (b), $2\theta = 11.7°, 23.5°, 35.4°, 47.8°$ ($CsPb_2Br_5$, denoted by ⬟), $2\theta = 13.5°$ (Pb_2OCO_3, denoted by ◆), $2\theta = 27.3°$ ($PbBr_2$, denoted by ●) and $2\theta = 28.8°$ (PbO, denoted by ▼).

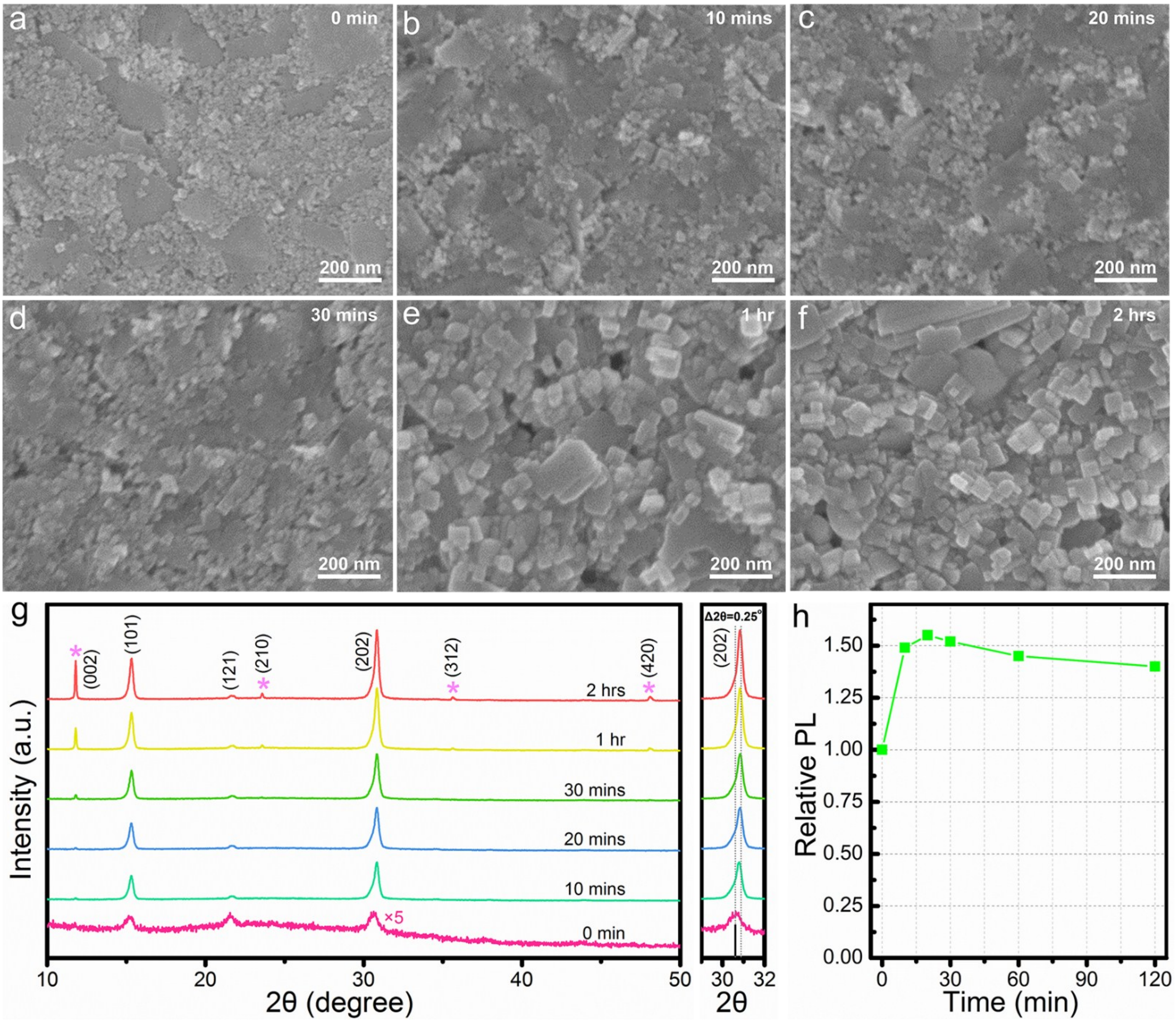

Fig. S10 (a-f) Typical SEM images of dual phase $CsPbBr_3$-$CsPb_2Br_5$ NCs films after annealing for different time at 200 ºC. (g) *Ex situ* PXRD patterns of dual phase $CsPbBr_3$-$CsPb_2Br_5$ NCs films annealed for different time at 200 ºC. The pink star denoted the peaks of $CsPb_2Br_5$. Inset shows a subtle yet monotonic shift of the (202) peak toward higher degree, which is the result of progressive lattice contraction as the annealing time increasing. (h) The PL intensity variation as a function of annealing time at 200 ºC.

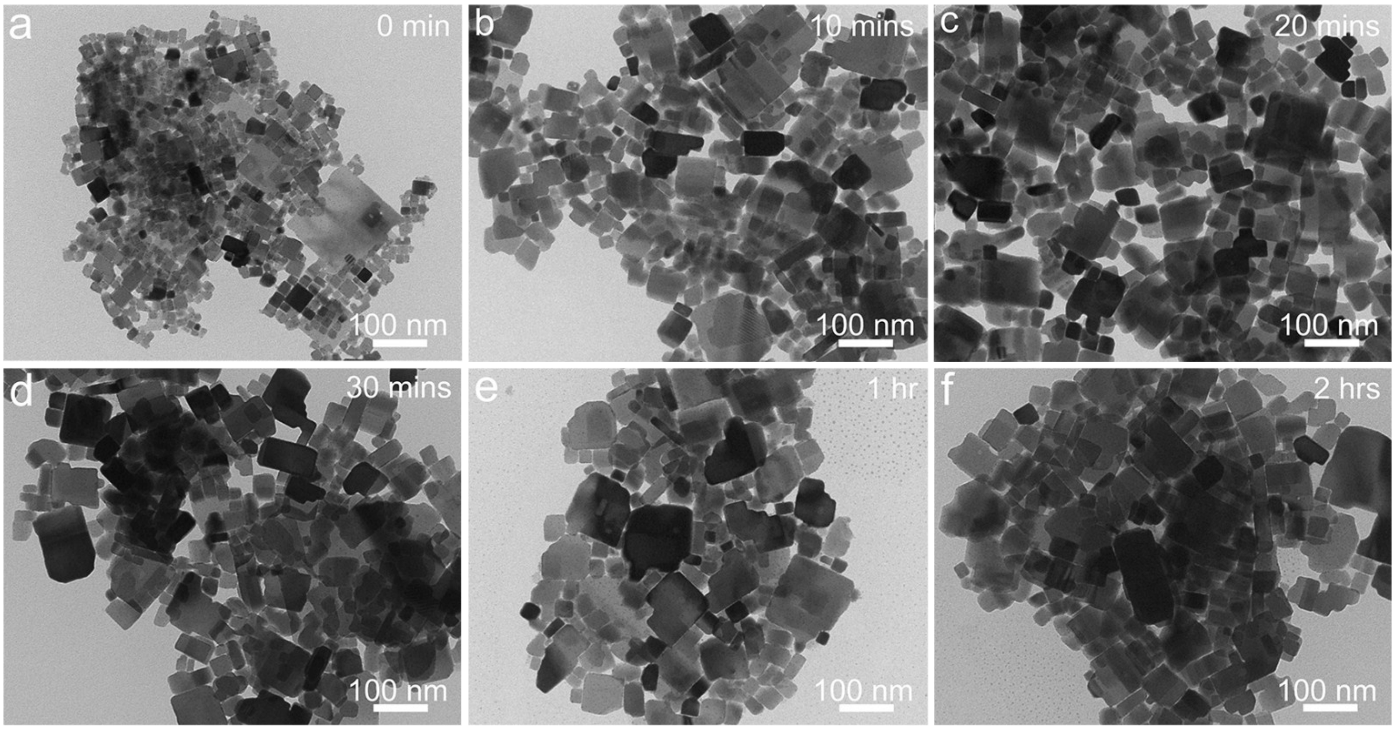

Fig. S11 Typical TEM images of dual phase $CsPbBr_3$-$CsPb_2Br_5$ NCs films after annealing for different time at 200 ºC.

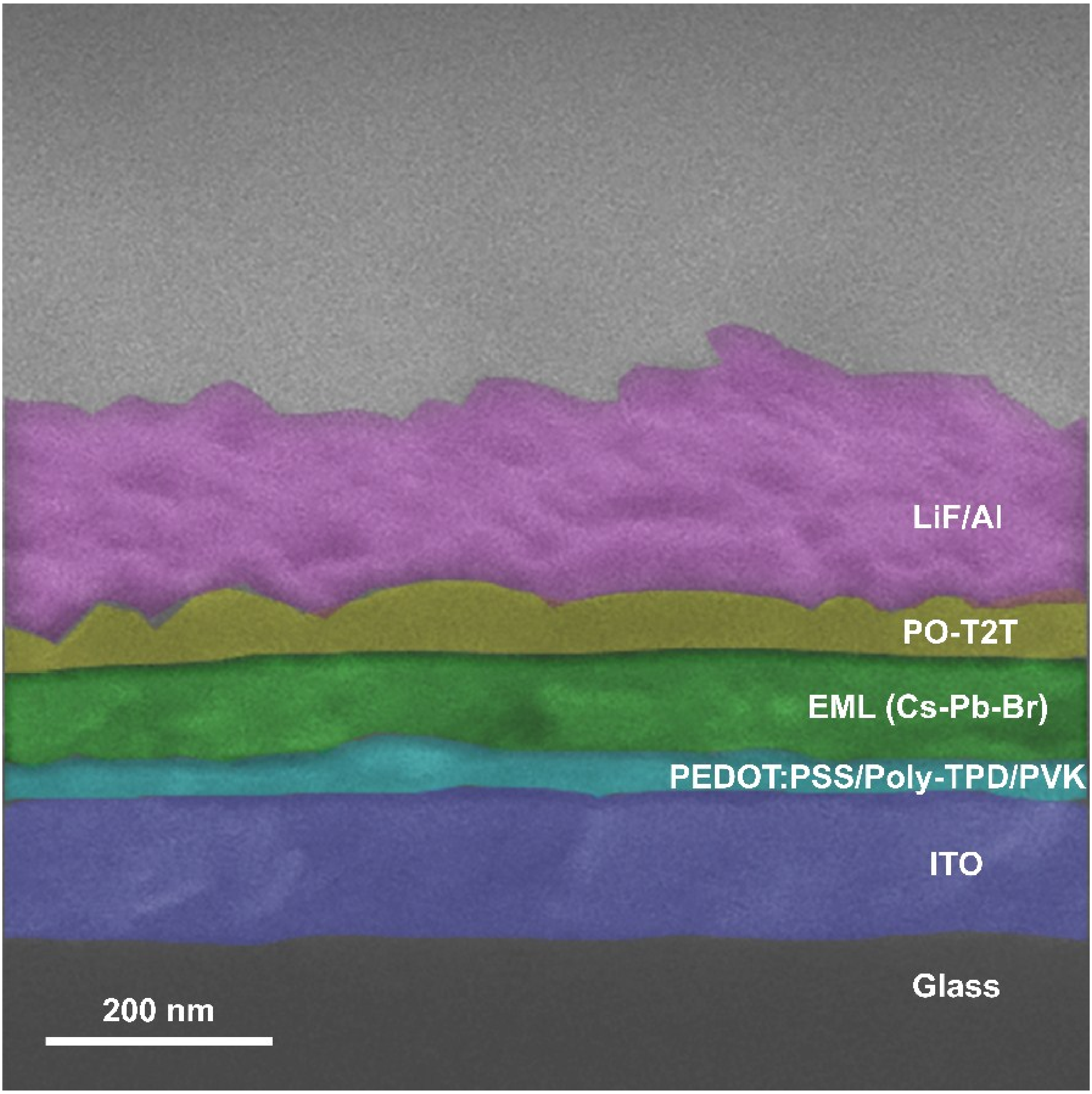

Fig. S12 Cross-sectional SEM image for the dual phase $CsPbBr_3$-$CsPb_2Br_5$ NCs based PeLED showing the multilayer structure.

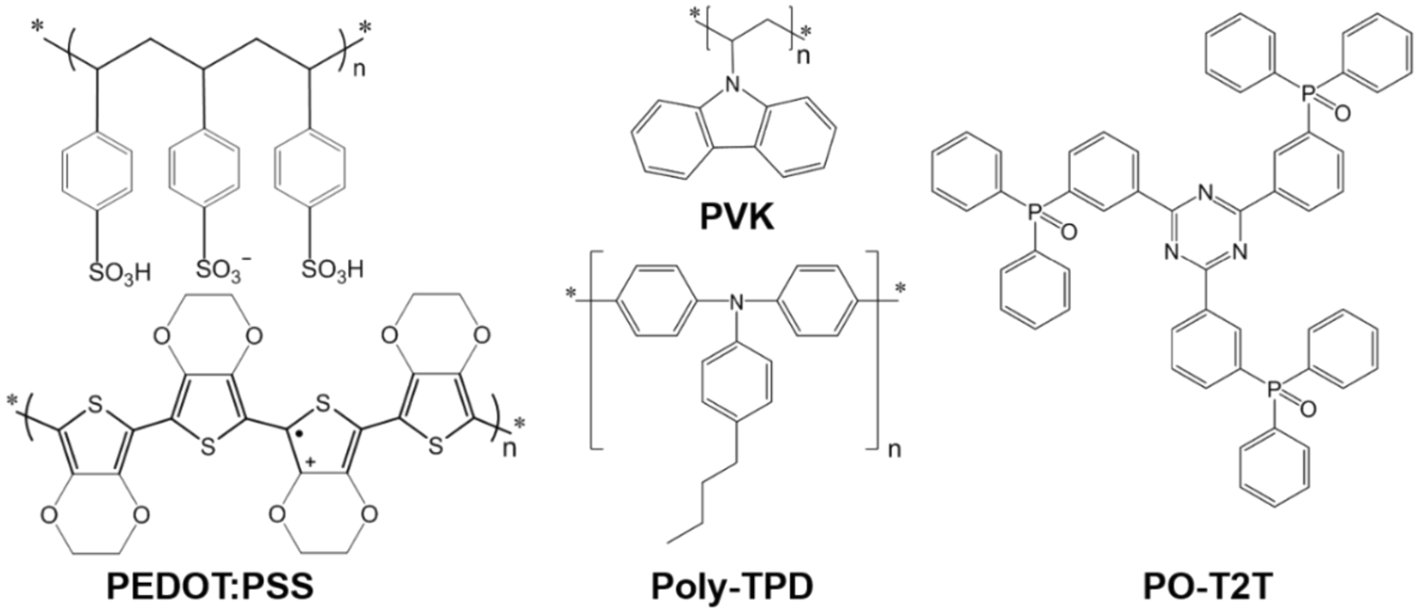

Fig. S13 Molecular structures of various organic materials, including hole injection layer (PEDOT : PSS), hole transporting layer (PVK, Poly-TPD), and electron transporting layer (PO-T2T).

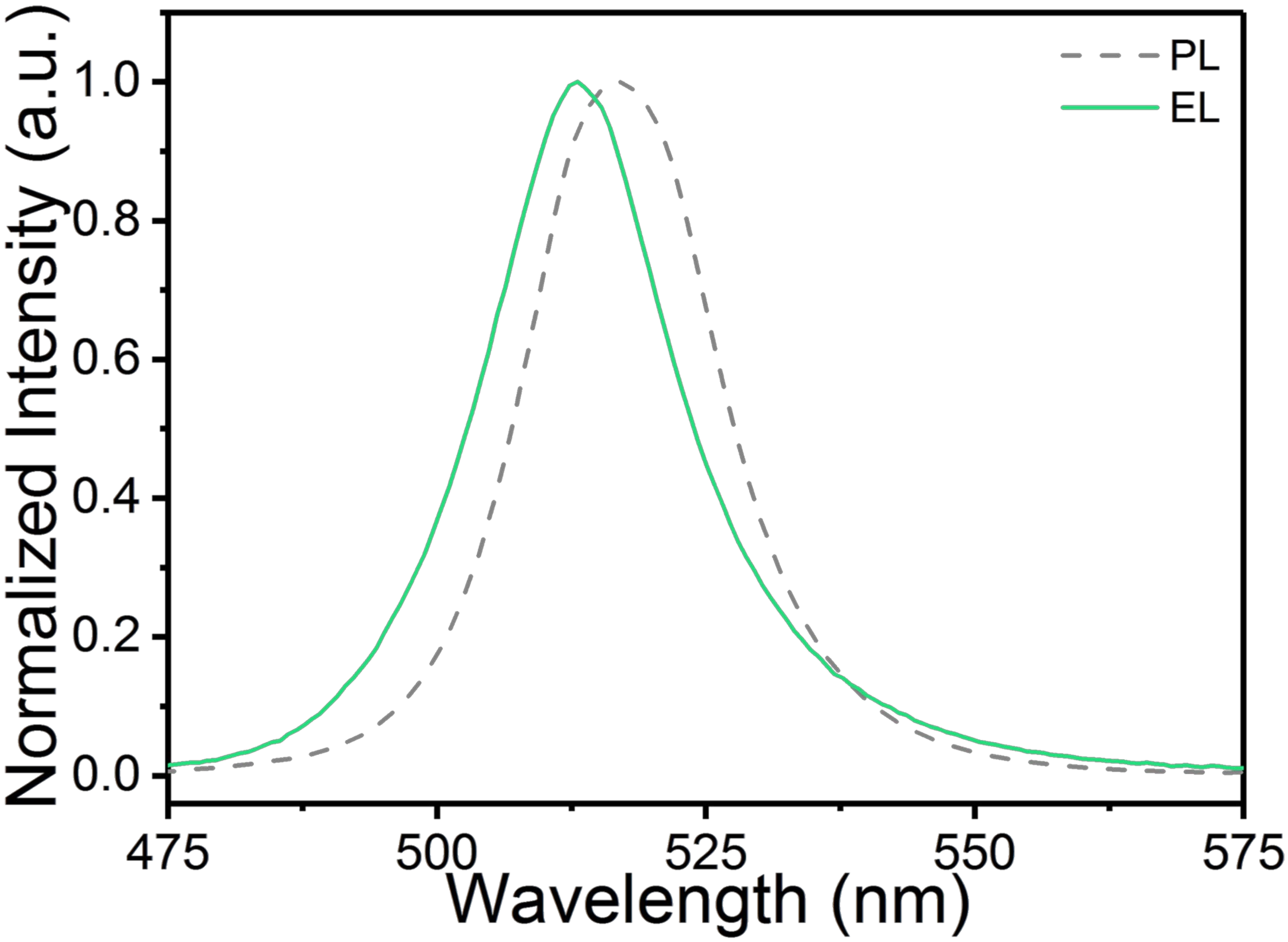

Fig. S14 PL spectrum of the dual phase $CsPbBr_3$-$CsPb_2Br_5$ NCs film, and EL spectrum of as-fabricated PeLED.

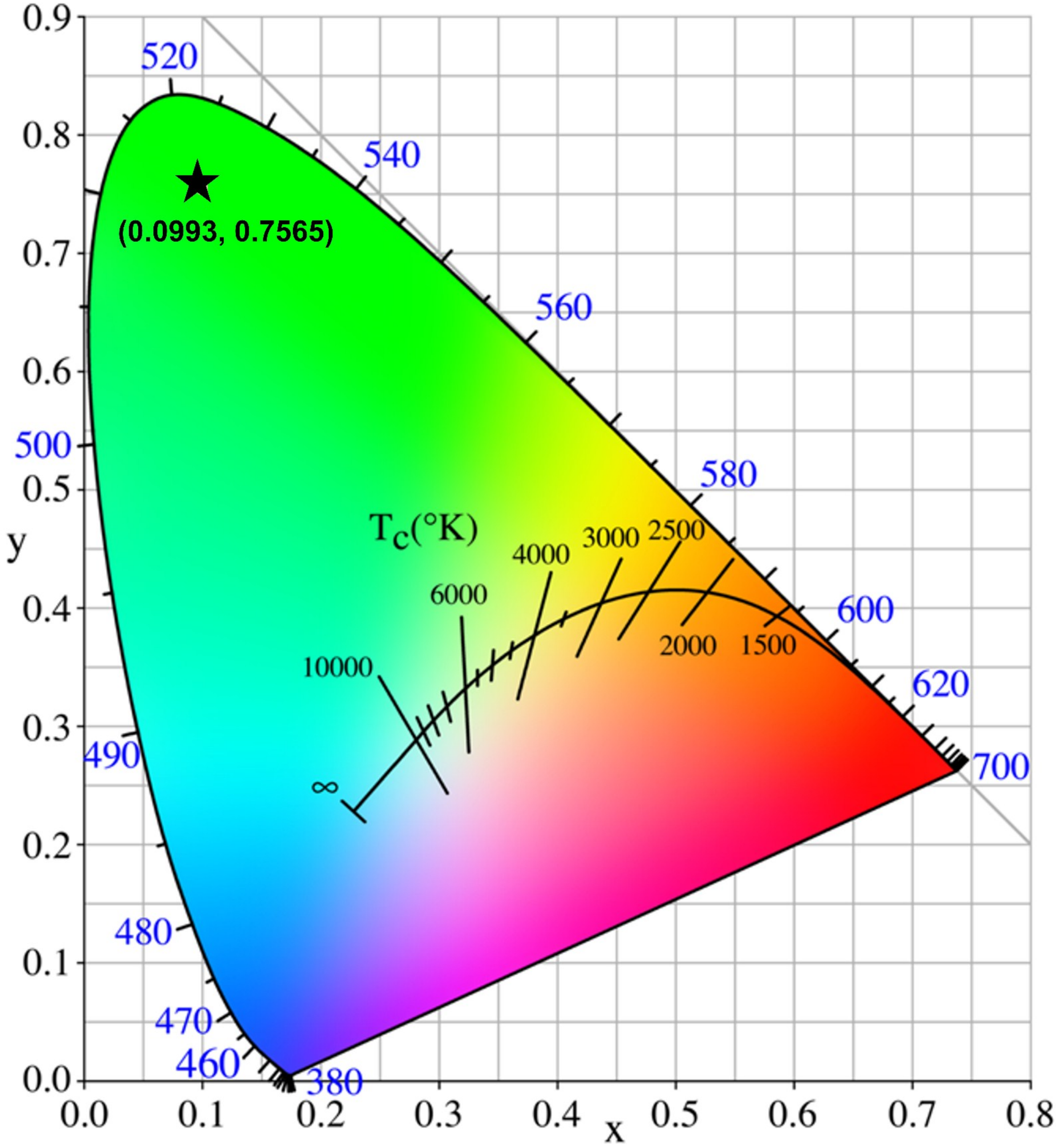

Fig. S15 Commission Internationale de l'Eclairage (CIE) chromaticity coordinates for the dual phase $CsPbBr_3$-$CsPb_2Br_5$ NCs based PeLED in this work.

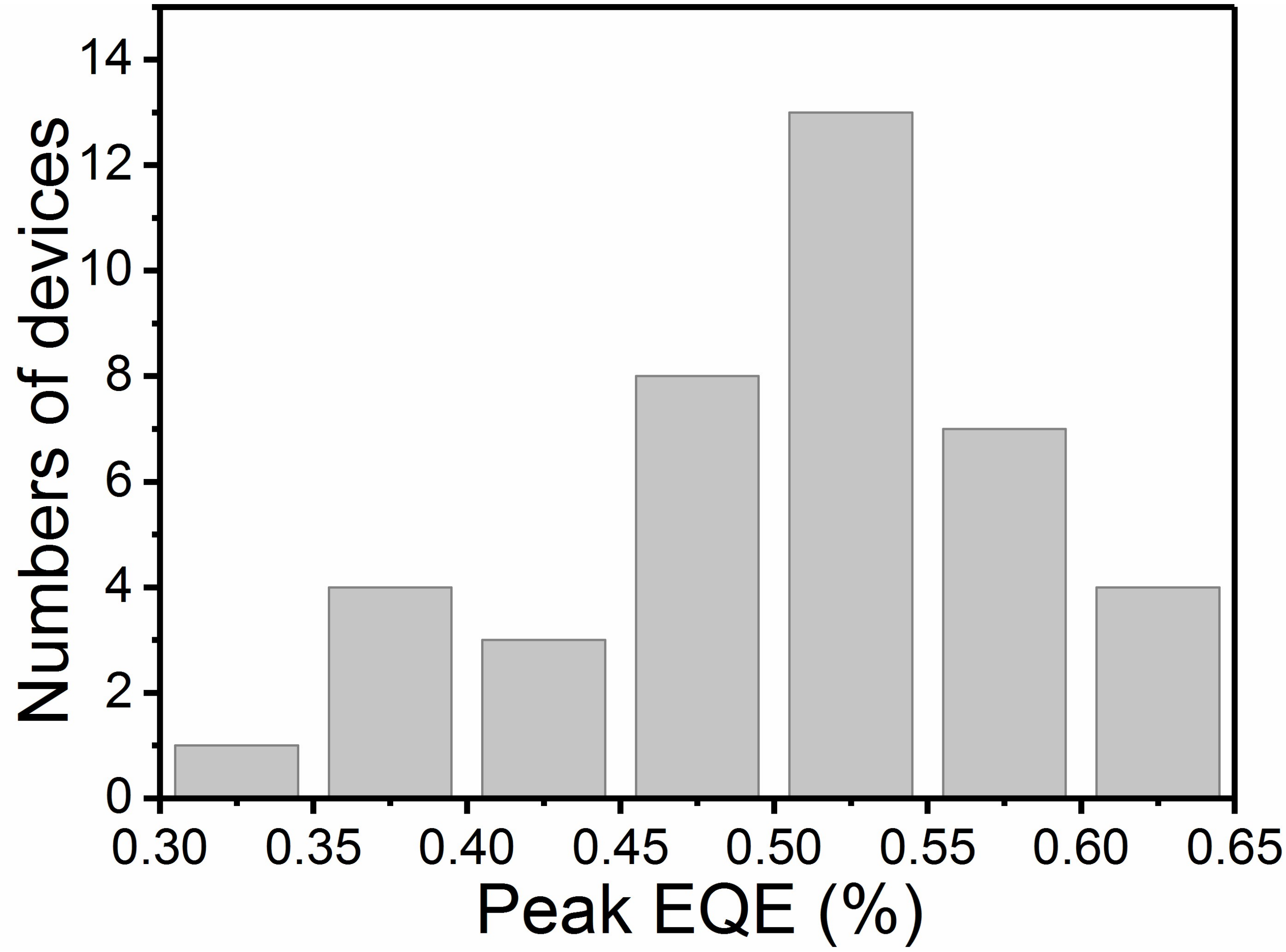

Fig. S16 EQE distribution of dual phase $CsPbBr_3$-$CsPb_2Br_5$ NCs based PeLED. The statistical results are based on 40 devices.

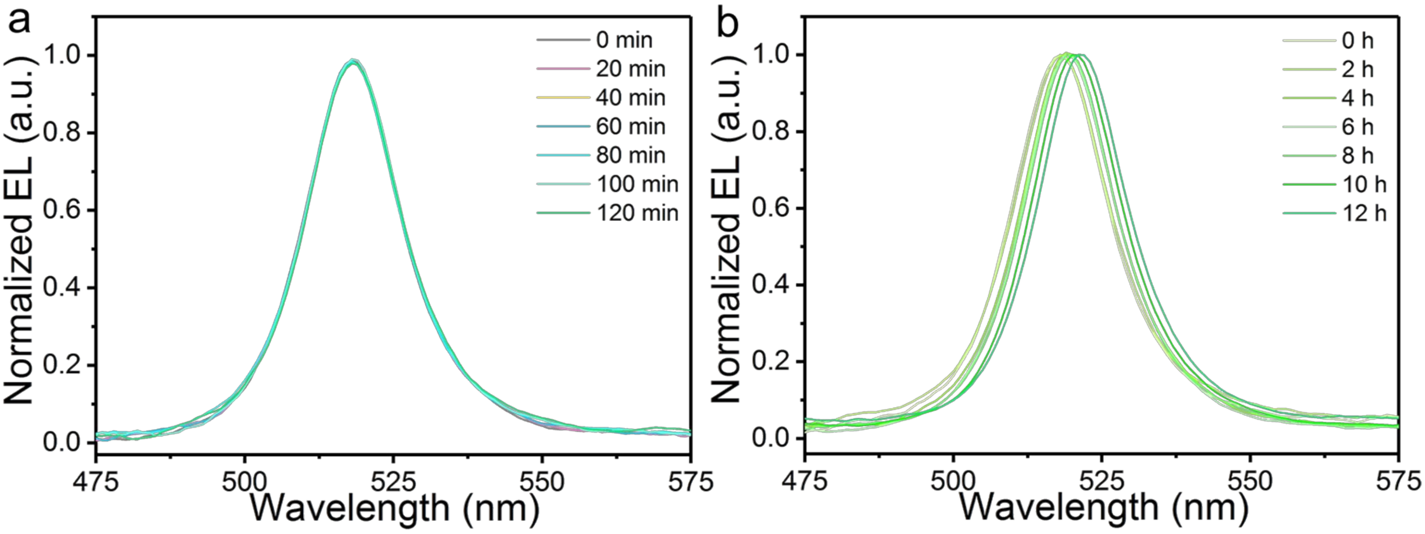

Fig. S17 Normalized EL spectral stability of PeLED devices ($CsPbBr_3$-$CsPb_2Br_5$ NCs) continuously operated under 5.5 V within 2 h (a) and 12 h (b), respectively. The EL spectra of dual phase $CsPbBr_3$-$CsPb_2Br_5$ NCs based device remained almost identical under continuous operation at 5.5 V within 2 hours. Even after 12 hours, only a slight red-shift of 3 nm in EL peak and 2 nm decrease in the FWHM are recorded.

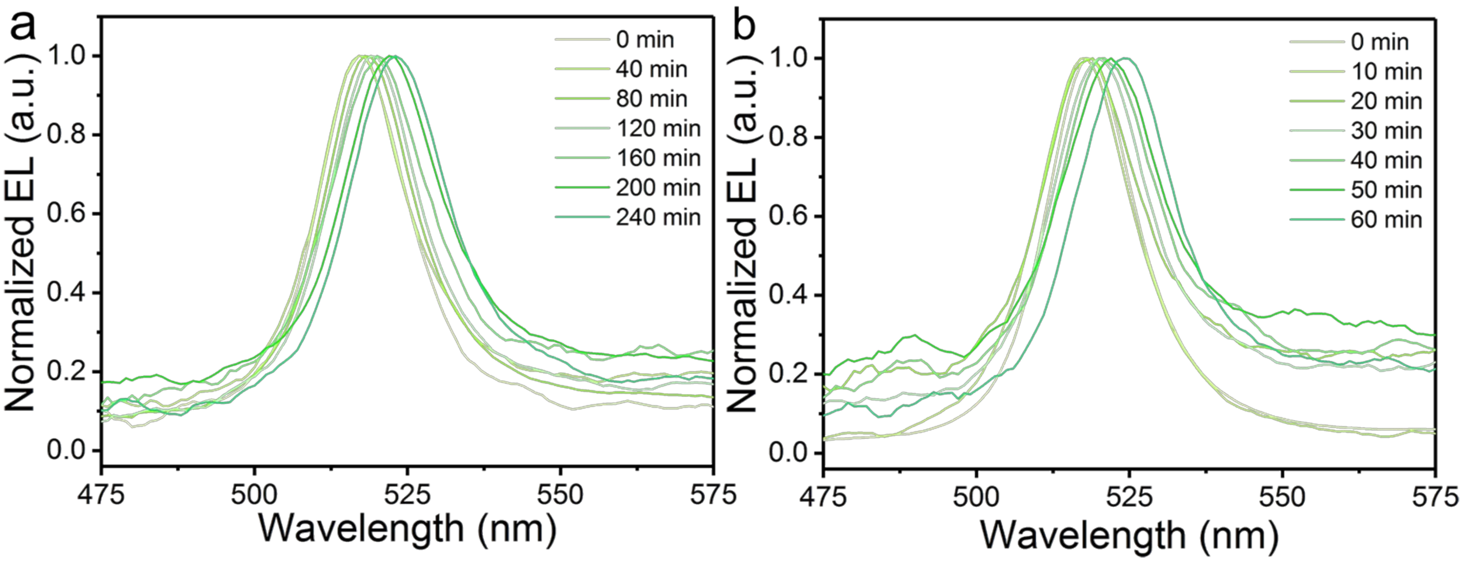

Fig. S18 Normalized EL spectra of devices based on HI (a) or LARP-SP (b) under 5.5 V continuous operation.

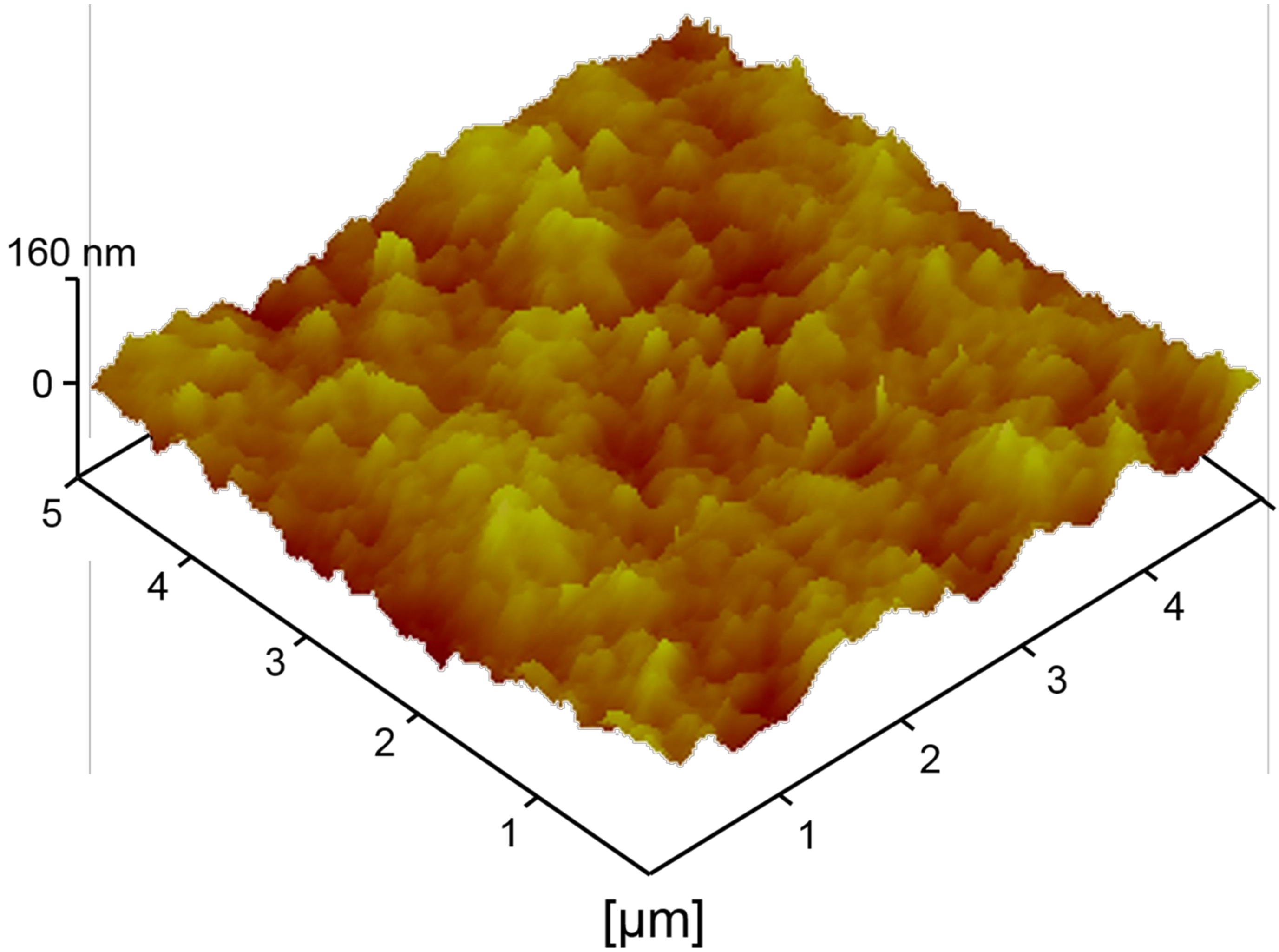

Fig. S19 Atomic force microscopy (AFM) characterization of the dual phase $CsPbBr_3$-$CsPb_2Br_5$ NCs film showing its rough surface.

References

1 J. Pan, L. N. Quan, Y. B. Zhao, W. Peng, B. Murali, S. P. Sarmah, M. J. Yuan, L. Sinatra, N. M. Alyami, J. K. Liu, E. Yassitepe, Z. Y. Yang, O. Voznyy, R. Comin, M. N. Hedhili, O. F. Mohammed, Z. H. Lu, D. H. Kim, E. H. Sargent and O. M. Bakr, *Adv. Mater.*, 2016, **28**, 8718.

2 S. B. Sun, D. Yuan, Y. Xu, A. F. Wang and Z. T. Deng, *Acs Nano*, 2016, **10**, 3648.

3 J. W. Xu, W. X. Huang, P. Y. Li, D. R. Onken, C. C. Dun, Y. Guo, K. B. Ucer, C. Lu, H. Z. Wang, S. M. Geyer, R. T. Williams and D. L. Carroll, *Adv. Mater.*, 2017, **29**, 1703703.

4 H. Cho, C. Wolf, J. S. Kim, H. J. Yun, J. S. Bae, H. Kim, J. M. Heo, S. Ahn and T. W. Lee, *Adv. Mater.*, 2017, **29**, 1700579.

5 J. Pan, L. N. Quan, Y. B. Zhao, W. Peng, B. Murali, S. P. Sarmah, M. J. Yuan, L. Sinatra, N. M. Alyami, J. K. Liu, E. Yassitepe, Z. Y. Yang, O. Voznyy, R. Comin, M. N. Hedhili, O. F. Mohammed, Z. H. Lu, D. H. Kim, E. H. Sargent and O. M. Bakr, *Adv. Mater.*, 2016, **28**, 8718.

6 J. H. Li, L. M. Xu, T. Wang, J. Z. Song, J. W. Chen, J. Xue, Y. H. Dong, B. Cai, Q. S. Shan, B. N. Han and H. B. Zeng, *Adv. Mater.*, 2017, **29**, 1603885.

7 X. L. Zhang, B. Xu, J. B. Zhang, Y. Gao, Y. J. Zheng, K. Wang and X. W. Sun, *Adv. Funct. Mater.*, 2016, **26**, 4595.

8 C. J. Qin, T. Matsushima, A. S. D. Sandanayaka, Y. Tsuchiya and C. Adachi, *J. Phys. Chem. Lett.*, 2017, **8**, 5415.

9 J. Z. Song, J. H. Li, L. M. Xu, J. H. Li, F. J. Zhang, B. N. Han, Q. S. Shan and H. B. Zeng, *Adv. Mater.*, 2018, **30**, 1800764.

10 S. Wei, Y. C. Yang, X. J. Kang, L. Wang, L. J. Huang and D. C. Pan, *Inorg. Chem.*, 2017, **56**, 2596.

11 X. Y. Zhang, X. Bai, H. Wu, X. T. Zhang, C. Sun, Y. Zhang, W. Zhang, W. T. Zheng, W. W. Yu and A. L. Rogach, *Angew. Chem., Int. Ed.*, 2018, **57**, 3337.